

# Selective Photothermolysis of Lipid-Rich Tissues: A Free Electron Laser Study

R. Rox Anderson, MD,<sup>1\*</sup> William Farinelli, BA,<sup>1</sup> Hans Laubach, MD,<sup>1</sup> Dieter Manstein, MD, PhD,<sup>1</sup> Anna N. Yaroslavsky, PhD,<sup>1</sup> Joseph Gubeli III, MS,<sup>2</sup> Kevin Jordan, PE,<sup>2</sup> George R. Neil, PhD,<sup>2</sup> Michelle Shinn, PhD,<sup>2</sup> Walter Chandler, MD,<sup>2</sup> Gwyn P. Williams, PhD,<sup>2</sup> Steven V. Benson, PhD,<sup>2</sup> David R. Douglas, PhD,<sup>2</sup> and H.F. Dylla, PhD<sup>2</sup>

<sup>1</sup>Wellman Center for Photomedicine, Harvard Medical School, Boston, Massachusetts

<sup>2</sup>Thomas Jefferson National Accelerator Facility, Newport News, Virginia

**Background and Objectives:** In theory, infrared vibrational bands could be used for selective photothermolysis of lipid-rich tissues such as fat, sebaceous glands, or atherosclerotic plaques.

**Study Design/Materials and Methods:** Absorption spectra of human fat were measured, identifying promising bands near 1,210 and 1,720 nm. Photothermal excitation of porcine fat and dermis were measured with a 3.5–5  $\mu$ m thermal camera during exposure to the free electron laser (FEL) at Jefferson National Laboratory. Thermal damage to full-thickness samples exposed at  $\sim$ 1,210 nm through a cold contact window, was assessed by nitrobluetetrazolium chloride staining *in situ* and by light microscopy.

**Results:** Photothermal excitation of fat was twice that of dermis, at lipid absorption bands (1,210, 1,720 nm). At 1,210 nm, a subcutaneous fat layer several mm thick was damaged by FEL exposure, without apparent injury to overlying skin.

**Conclusion:** Selective photothermal targeting of fatty tissues is feasible using infrared lipid absorption bands. Potential clinical applications are suggested by this FEL study. *Lasers Surg. Med.* 38:913–919, 2006.

© 2006 Wiley-Liss, Inc.

**Key words:** dermis; fat; tissue optics

## INTRODUCTION

Selective photothermolysis (SP) is a widely used treatment approach that preferentially heats tissue “targets,” which absorb a pulse of optical radiation more strongly than surrounding tissues [1]. Both source and tissue factors affect SP. In general, the source wavelength region and beam optics are chosen to produce preferential absorption in the desired targets; and pulse duration or exposure time is chosen to be nearly equal to the thermal relaxation time of the desired target structures [2]. Cooling at the tissue surface can be employed before, during, and/or after light delivery to prevent thermal injury of a superficial tissue layer [3]. Since its conception over 20 years ago, SP has been developed clinically for treating microvascular skin malformations [4], pigmented lesions [5], tattoos [6], pigmented hair [7], glaucoma [8], laryngeal lesions [9], and other conditions. In all of these applications, visible or

near-infrared lasers or intense pulsed light sources are used to pump electronic absorption transitions of the tissue “pigments” hemoglobin, oxyhemoglobin, melanin, or tattoo inks.

SP has not yet been developed using infrared vibrational absorption bands. The far-infrared is known as a ‘molecular fingerprint’ spectral region because strong, narrow vibrational modes are characteristic of chemical bond structures. While in theory SP could be performed using far-infrared pulses, the utility of wavelengths greater than about 2,500 nm is limited because strong absorption by water prevents photons from penetrating more than about 0.1 mm into tissue. In contrast, the near- and mid-infrared spectral region of about 900–2,800 nm includes the most tissue-penetrating optical wavelengths, specifically around 1,200 nm. In this spectral region, absorption is low because the photon quantum energy is less than electronic transition energy in most organic molecules, and optical scattering is weak [10]. In this region, there are multiple weak vibrational absorption bands, consisting of overtones of the fundamental modes responsible for strong far-infrared absorption.

In this study, we investigate the potential for SP of lipid-rich tissues, by pumping vibrational absorption bands. Lipids contain copious CH and CH<sub>2</sub> bonds. Lipid-rich tissues usually have low water content compared with other soft tissues. Therefore, one part of our strategy for SP of lipid-rich tissues, is to use lipid vibrational bands that lie “in between” the dominant absorption bands of water [11].

---

The authors certify that they have no affiliation with or financial involvement in any organization or entity with a direct financial interest in the subject matter or material discussed in the manuscript.

Contract grant sponsor: Department of Defense; Contract grant number: FA 9550-04-1-0079; Contract grant sponsor: Office of Naval Research; Contract grant sponsor: Commonwealth of Virginia.

\*Correspondence to: Prof. R. Rox Anderson, MD, Director, Wellman Center for Photomedicine, BHX-630, Massachusetts General Hospital, Boston, MA 02114.

E-mail: RRAnderson@partners.org

Accepted 11 July 2006

Published online 18 December 2006 in Wiley InterScience (www.interscience.wiley.com).

DOI 10.1002/lsm.20393

Initially we measured infrared spectra of human fat and water, and noted three bands near 915, 1,210, and 1,720 nm for which absorption by fat exceeds that of water. It was also noted that heat capacity and thermal conductivity are lower in fatty tissues, which tend to favor heating of fat [12]. We then created a Monte-Carlo model of tissue optics and photothermal excitation of fat and sebaceous glands in situ. When delivered with pre-cooling and parallel cooling at the skin surface [3], the 1,210 nm band was predicted to be capable of selectively targeting both subcutaneous fat and sebaceous glands. Commercially available diode, Nd:YLF and other lasers in this spectral region are limited to several watts and/or are not wavelength tunable, but a preliminary study was performed and reported using a low power, Raman-shifted Nd fiber laser [13]. Conventional sources with sufficient power that can be tuned around these wavelengths are lacking. Therefore, we used the high power superconducting free electron laser (FEL) at the Jefferson National Accelerator Laboratory to study the potential for SP of lipid-rich tissues. Photothermal excitation spectra were taken around the 1,210 and 1,720 nm bands. We then demonstrated SP of porcine subcutaneous fat exposed to the FEL near 1,210 nm, through the intact overlying epidermis and dermis.

## MATERIALS AND METHODS

### Absorption Spectra

Human subcutaneous fat obtained from surgically discarded normal tissue from the chest of an adult male was frozen, thawed, then carefully dissected to exclude dermis, vessels, and hair follicles. The fat was heated to 45°C and gently squeezed against 0.2  $\mu\text{m}$  pore size filter paper to obtain a clear, yellow liquid from lysis of adipocytes. Visually, the filtered fat samples were completely clear (had no apparent turbidity); still, an integrating sphere spectrophotometer was employed to reduce the potential influence of scattering on measured absorption spectra. The absorption spectrum of this material, and of distilled deionized water, was taken from 800 to 2,600 nm in 1 mm and 1 cm quartz cuvettes placed at the entrance port of a dual beam integrating sphere spectrophotometer (UV5270, Beckman Instruments, CA). The fat sample was maintained at 35–40°C during measurement, to avoid turbidity.

### Tissue and Other Samples

Full-thickness abdominal skin ( $\sim 3$  mm dermis thickness) with attached, intact subcutaneous fat (5–10 mm thickness) was obtained fresh from outbred farm pigs. Samples used for photothermal spectroscopy with the FEL were flash frozen and then thawed prior to use. Samples used for FEL exposures to create thermal lesions in the tissue, were kept on ice without freezing to avoid artifacts, then used fresh. Aqueous gels prepared using 6% (w:w) gelatin (Knox, Kraft Foods, Tarrytown NY) in 50 mm diameter plastic petri dishes were used for comparison of photothermal excitation by FEL with the expected behavior of water. Fresh lard (porcine fat) placed in a 50 mm petri dish was also used for comparison.

### Free Electron Laser (FEL)

The Jefferson National Laboratory FEL was employed as a source for both photothermal excitation measurements, and for exposure of tissue samples in vitro. Briefly, this FEL is driven by a superconducting electron accelerator achieving  $\sim 115$  MeV electron bunches, which after passing through an adjustable magnetic “wiggler” to induce relativistic photon emission in the laser cavity, are decelerated by passing out of phase through the same accelerator. This “recycles” most of the electron energy, achieving high overall electron-to-photon energy efficiency. Average power output of this FEL can be as high as 10 kW. For our experiments, metal cavity mirrors were used to allow broad wavelength tuning, which limited the FEL average output power to a range of approximately 30–100 W. Time structure of the FEL output consists of an up to 75 MHz train of  $\sim 400$  femtoseconds micropulses, such that the peak-to-average power ratio is approximately  $3 \times 10^4$ . In our experiments, the FEL beam was defocused and delivered to the tissue samples in large exposure spots. Under these conditions, thermal excitation of the tissue is insensitive to the presence of FEL micropulses, equivalent to a continuous beam at the same average power. The femtosecond micropulses impose a bandwidth limit on the FEL. Spectrometer scans were obtained at each wavelength used, to determine the FEL center wavelength and bandwidth. Bandwidth was typically 15–25 nm (FWHM), with an approximately Gaussian spectral shape. Between experimental runs several months apart, the FEL wiggler and cavity were changed, such that the beam power profile was Gaussian for most of our photothermal excitation measurements, and was a flat profile for the tissue exposures used to create thermal lesions.

### Photothermal Excitation Measurements

FEL-induced temperature rise was measured at the surface of tissue and other samples, by photothermal radiometry using a commercial thermal camera (PM180 Thermacam, FLIR Systems, Inc., N. Billerica MA) sensitive to 3.5–5  $\mu\text{m}$  blackbody radiation from the sample surface. The thermal camera was blind at the FEL wavelengths used in this study. The thermal camera was commercially calibrated prior to the study, and calibration was verified by obtaining the correct temperature of water samples within  $\pm 1^\circ\text{C}$ . Camera software includes peak-temperature detection at the center of the field of view, which was aligned with the center of the FEL beam incident upon a sample's surface. Samples were placed horizontally on a movable stage, with the FEL beam axis normal to the sample surface, and the thermal camera viewing axis  $\sim 15^\circ$  from normal. FEL exposure energy was sampled using a  $\sim 1\%$  beamsplitter and energy meter (12A-SH-V1, Ophir Optonics, Inc., Wilmington MA) that allowed the energy delivered by each FEL exposure to be determined. A lens was used to adjust the FEL beam diameter reaching the sample over a range of approximately 6–22 mm. FEL exposure duration was controlled at the accelerator level, by adjusting the electron source duration. For

photothermal excitation measurements, FEL exposures were typically in the range of 50–250 milliseconds.

Photothermal excitation of each tissue sample was performed without allowing the tissue temperature to ever exceed 50°C, that is, without causing significant tissue thermal damage. For each sample, a range of FEL wavelengths were investigated. The delivered FEL beam energy was determined for each individual exposure. Photothermal excitation was normalized for beam energy by dividing each exposure's induced peak temperature rise of the sample, by the associated FEL exposure fluence (result expressed in °C/J cm<sup>2</sup>). The results of at least five independent FEL exposures per sample were used to determine mean and standard deviation of photothermal excitation at each wavelength, for each sample. The samples tested in this manner included intact porcine fat, intact porcine skin, aqueous gels, and lard. FEL wavelength was tuned to discrete values from 1,200 to 1,330 nm, and from 1,600 to 1,800 nm.

### Tissue Exposures

Whole, intact skin-and-fat tissue samples were exposed to FEL under conditions intended to test the hypothesis that preferential photothermal damage of subcutaneous fat was possible, without apparent damage to the overlying skin. Even at wavelengths such as ~1,210 nm which exhibited preferential photothermal excitation of fat, skin surface cooling is necessary to prevent unwanted thermal injury to the dermis. An apparatus was used that mimics the temperature gradient obtained by skin cooling with cold contact windows *in vivo*. Samples with at least 5 mm of subcutaneous fat were used. The copper stage upon which samples were placed, was maintained at 37°C. A cold sapphire window (3 mm × 50 mm diameter) was mounted in thermal contact with a copper block through which ice water was passed by means of a small pump. The cold sapphire window temperature was 6–8°C. Tissue samples ~2 cm in diameter were gently squeezed between the cold sapphire window in contact with the epidermal side, and the warm base in contact with the deep fat margin. Prior to FEL exposure, the sample was allowed to equilibrate for at least 30 seconds. These thermal conditions mimic those of compressive contact cooling *in vivo*.

FEL exposures of tissue samples were performed at the lipid-selective wavelength of 1,214 nm (FEL bandwidth 17 nm FWHM), and for comparison under identical conditions at the non-lipid-selective wavelength of 1,250 nm. Water has nearly the same absorption coefficient at these two wavelengths, whereas fat absorbs more than twice as strongly at 1,210 nm. For tissue damage studies, the FEL exposure duration was 16 seconds, the exposure beam profile was nearly uniform, and beam diameter was either 8, 11, or 17 mm. At each wavelength, 12 samples were exposed to a range of FEL power densities in order to ensure sub-threshold, near-threshold, and above-threshold exposures for thermal damage to the sample.

### Tissue Damage Assessment

Tissue samples exposed to FEL and unexposed control tissue samples, were vertically bisected with a razor blade through the optical exposure axis. One half was fixed in formalin and processed routinely for light microscopy after staining with hematoxylin and eosin. The other half was incubated for 15 minutes at room temperature in a solution containing nitroblue tetrazolium chloride (NBTC) as previously described [14]. Briefly, NBTC is a colorless substrate for mitochondrial enzymes, notably NADPH diaphorase, producing a dark blue reporter dye for enzyme activity. Thermal denaturation causes loss of enzyme activity (loss of NBTC staining), that correlates well with cell lethality. Digital photographs were taken of the bisection surface corresponding to a vertical section along the FEL beam axis, after NBTC staining.

## RESULTS

### Absorption Spectroscopy

Absorption spectra of human fat extract and water are shown in Figure 1. Over most of the spectrum, absorption by water greatly exceeds that of fat. At lipid absorption bands near 1,210 and 1,720 nm, absorption by fat is greater than that of water.

### Photothermal Excitation Measurements

For adiabatic heating, a temperature rise of  $\Delta T = \mu_a F / (\rho c)$  is expected [1], where  $\mu_a$  is the optical absorption coefficient,  $F$  is local fluence within the sample,  $\rho$  is density, and  $c$  is specific heat capacity. It has been shown by pulsed photothermal radiometry, that optical scattering and internal reflection of back-scattered light somewhat increases the value of  $F$  near the surface of turbid samples such as skin [15]. Photothermal excitation data for aqueous gels and lard are shown in Figure 2, as  $\Delta T / F_0$ , where  $F_0$  is the incident FEL fluence. In this study, the absolute calibration error of the incident FEL fluence is estimated

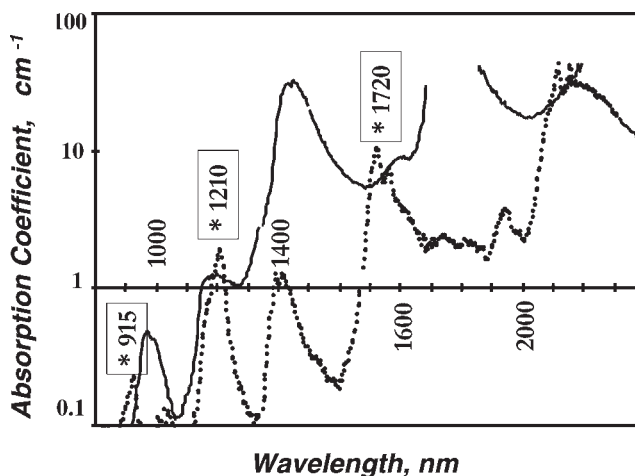


Fig. 1. Infrared absorption spectra of water (solid line) and human fat (dotted line), noting approximate wavelengths of fat absorption maxima.

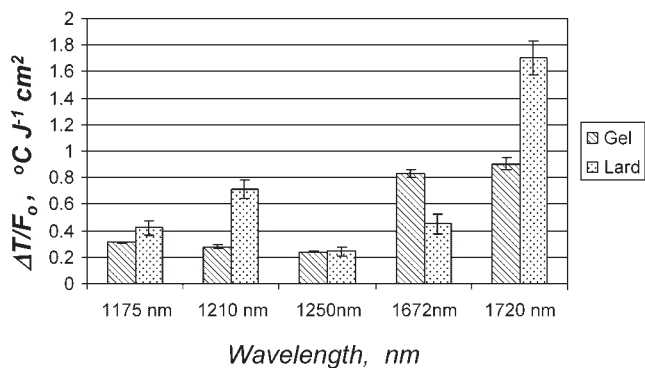


Fig. 2. FEL-induced photothermal excitation of water (93% aqueous gel) and porcine fat (lard) at selected wavelengths, corrected for FEL fluence by plotting  $\Delta T/F_0$ , where  $F_0$  is the incident FEL fluence and  $\Delta T$  is the peak temperature rise (see text).

to be up to  $\pm 50\%$  due to the combined uncertainties of energy measurement ( $\sim 10\%$ ), beam profile variations ( $\sim 10\%$ ), and exposure spot size ( $\sim 30\%$  uncertainty in exposure area). Optically and thermally, the simplest sample in this study was aqueous gel, for which  $\mu_a$  and  $\rho c$  are well known, and for which optical scattering is negligible. The aqueous gel photothermal excitation measurements therefore allow an independent check of the FEL fluence calibration. Measured values of  $\Delta T/F_0$  for aqueous gels were close to those expected from  $\mu_a/(\rho c)$  for water at the FEL wavelengths tested. At 1,210 nm,  $\mu_a/(\rho c)$  for water is  $0.25^\circ\text{C}/\text{J cm}^2$ , which corresponds well to the mean measured value of  $\Delta T/F_0$  of  $0.28^\circ\text{C}/\text{J cm}^2$  at this wavelength. At 1,720 nm,  $\mu_a/(\rho c)$  for water is  $1.4^\circ\text{C}/\text{J cm}^2$ , which corresponds to the mean measured value of  $\Delta T/F_0$  of  $0.90^\circ\text{C}/\text{J cm}^2$ .

Figure 3 shows photothermal excitation spectra for porcine fat and porcine skin, normalized to FEL pulse energy. At the  $\sim 1,210$  nm lipid absorption band, laser-induced heating of fat was approximately 2.2 times that of skin. At the  $\sim 1,720$  nm lipid absorption band, laser-induced heating of fat was approximately 1.7 times that of skin. Shape of the photothermal excitation spectra for dermis was consistent with water as the dominant optical absorber.

### Effects of FEL Exposures on Tissue

Loss of NBTC staining was apparent in the fresh tissue samples, clearly demarcating regions of thermal enzyme inactivation (Fig. 4). Exposure of fresh, intact, full-thickness porcine tissue samples at wavelengths near 1,210 nm (at which fat is preferentially excited), reproducibly caused thermal damage of subcutaneous fat with little or no injury to the overlying skin, over a range of FEL beam irradiances (Fig. 4A). The FEL exposure conditions found to reproducibly cause selective damage of subcutaneous fat were: center wavelength 1,206–1,214 nm (FEL bandwidth 17 nm FWHM), exposure duration 16 seconds delivered with parallel cooling as described above, exposure spot diameter

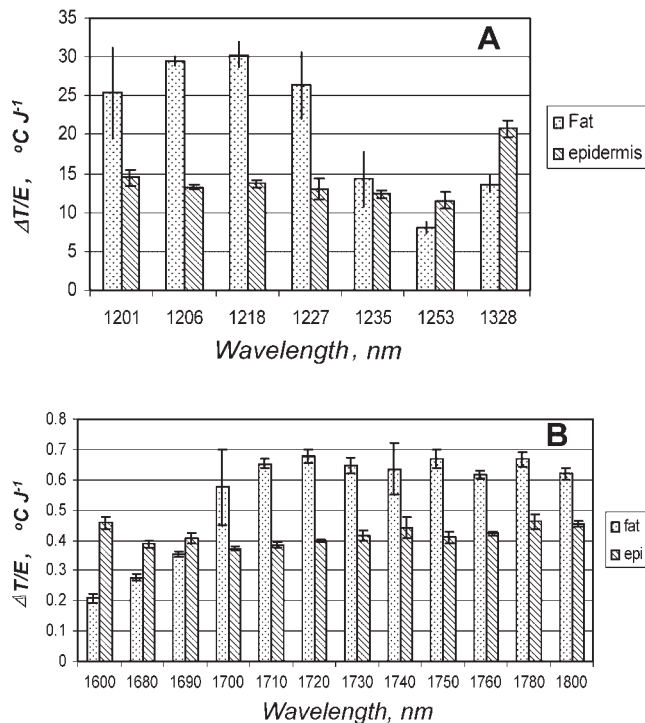


Fig. 3. FEL-induced photothermal excitation of porcine fat and porcine skin, normalized to FEL exposure energy (see text). Preferential heating of fat is maximum at the lipid absorption band maxima near 1,210 nm (A) and 1,720 nm (B). The data are consistent with water as the dominant absorber in skin and lipid as the dominant absorber in fat.

1.7 cm, FEL beam power 14–18 W (irradiance 6.2–8.0  $\text{W}/\text{cm}^2$ ; fluence 100–130  $\text{J}/\text{cm}^2$ ). Under the same conditions, FEL beam power  $\geq 20$  W produced injury to both fat and the deep dermis (Fig. 4B).

In contrast, exposure under identical sample set-up conditions at 1,250 nm (a nearby wavelength at which fat and dermis are equally excited), caused thermal damage of skin, with or without fat injury (Fig. 4C). Selective fat injury was not observed after 1,250 nm exposures at any FEL beam power. Peak temperature at the skin surface was monitored through the cold-contact sapphire window during these long exposures, by the thermal camera. At  $\sim 1,210$  nm, a peak skin surface temperature of 15–20°C was measured during exposures causing preferential fat injury. At  $\sim 1,250$  nm, exposures causing the same peak skin surface temperature range produced no apparent tissue damage, compared with unexposed controls. Dermal injury at either wavelength, was associated with measured peak skin surface temperatures  $> 20^\circ\text{C}$ .

Light microscopic examination of fixed sections stained with H&E, showed thermal injury in the same distributions as loss of NBTC staining in the (bisected) samples. After exposures at  $\sim 1,210$  nm in the irradiance range of 6–8  $\text{W}/\text{cm}^2$  delivered for 16 seconds, the epidermis and dermis appeared normal compared with unexposed control

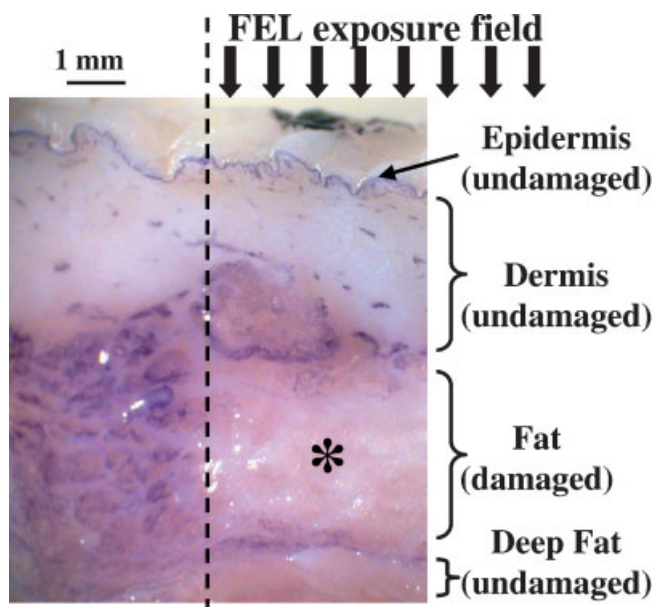


Fig. 4. Loss of nitroblue tetrazolium staining (\*) shows distribution of thermal damage, due to FEL-induced thermal inactivation of intracellular reductases (14). Preferential subcutaneous fat injury was reliably produced without dermal damage by wavelengths near 1,210 nm. Sample shown was exposed to 1,214 nm, 7.3 W/cm<sup>2</sup>, delivered through a cold sapphire window for 16 seconds, over a 1.7 cm diameter flat-field exposure spot. Adjacent fat and the overlying dermis and epidermis, were unaffected.

samples, while fibrous septae of the subcutaneous fat showed changes consistent with thermal denaturation. There was collagen fiber swelling with loss of demarcation, hyaline appearance, and the loss of birefringence typical for type I collagen thermal denaturation (Fig. 5). As with the NBTC staining, exposure to  $\sim 1,210$  nm at FEL irradiance  $\geq 20$  W/cm<sup>2</sup> caused injury to both fat and deep dermis. Exposures at 1,250 nm in the same irradiance range that caused selective fat injury at  $\sim 1,210$  nm, did not cause notable tissue damage. Whenever tissue effects were noted after 1,250 nm exposures, dermis was the primary site of injury. At high FEL irradiance of 20 W/cm<sup>2</sup>, 1,250 nm caused extensive thermal denaturation of the dermis and upper fat (Fig. 6).

## DISCUSSION

Our study takes several steps toward developing SP of fatty tissues. This is the first demonstration of SP based on vibrational, rather than electronic transitions. Previous studies of tissue ablation using FELs, have shown that far-infrared pulses absorbed by amide vibrational modes provide precise, efficient tissue removal [16]. The potential for laser-tissue interactions based on selective vibrational mode excitation deserves further study.

In this study, we identified the 1,210 and 1,720 nm absorption bands of lipids associated with CH<sub>2</sub> vibrational

modes, as useful for targeting lipid-rich structures. Using the 1,210 nm band, we showed that subcutaneous fat can be selectively damaged, up to at least 0.5 cm deep. Based on this work, conventional laser sources may potentially be designed with sufficient power at these wavelengths for medical applications. The 1,210 nm band in particular is interesting, as this is the most penetrating optical wavelength region. This band was also the most selective in this study for photothermal excitation of fat relative to dermis (see Fig. 3). The ability to affect subcutaneous fat with photons propagated through the dermis was initially somewhat surprising, because dermis also contains many organic molecules with CH and CH<sub>2</sub> bonds, in addition to a high water content. However, the 1,210 nm band is a high frequency overtone of R-CH<sub>2</sub>-R structures. Unlike the strong stretching modes of CH and OH near 3,000 nm that produce very high absorption in dermis, the strength of overtone bands is somewhat more dependent on details of molecular structure.

The size of targets amenable to SP varies from sub-cellular organelles, to large multicellular structures such as vessels and hair follicles. In general, exposure duration is chosen to be approximately equal to the thermal relaxation time of the target structure. In this study, we targeted the subcutaneous fat layer using very long (16 seconds) exposures that correspond to thermal confinement of an approximately 3 mm thick layer of adipose tissue. Long exposure time was also used to allow time for heat extraction from the overlying dermis during the FEL exposure. Without heat extraction by parallel cooling, dermal injury would have occurred at all of the FEL wavelengths studied.

Clinical applications of fat targeting by SP have yet to be developed, and there are many questions to be answered. This is true as well for other emerging schemes that target adipose tissue, including focused ultrasound, radiofrequency current, and the local injection of surfactants and other substances known as mesotherapy [17]. For example, are the targeted adipocytes removed without fibrosis or scarring during the healing process? Are the local stem cells capable of replacing the tissue? What temperatures and spatial distribution of temperature may be therapeutic? In this study we found that SP of fat *ex vivo* causes both cellular damage (loss of adipocyte NBTC staining) and extracellular matrix damage (loss of collagen birefringence in septae). For some potential applications, both may be useful. For example, "cellulite" is a common, acquired secondary sexual trait in women that involves both superficial collections of fat and architectural changes in the fibrous septae [18]. The primary locale for SP of subcutaneous fat is at and just below the dermis-fat junction. The potential for SP of fat as a treatment of cellulite is noted, but at this point entirely unknown.

The 1,210 nm waveband may also be useful for targeting sebaceous glands. SP of sebaceous glands was not optimized in this study, because these glands are small in porcine skin [19]. In contrast, human facial skin has large sebaceous glands that may be amenable to SP, for example, as a treatment for acne vulgaris, sebaceous

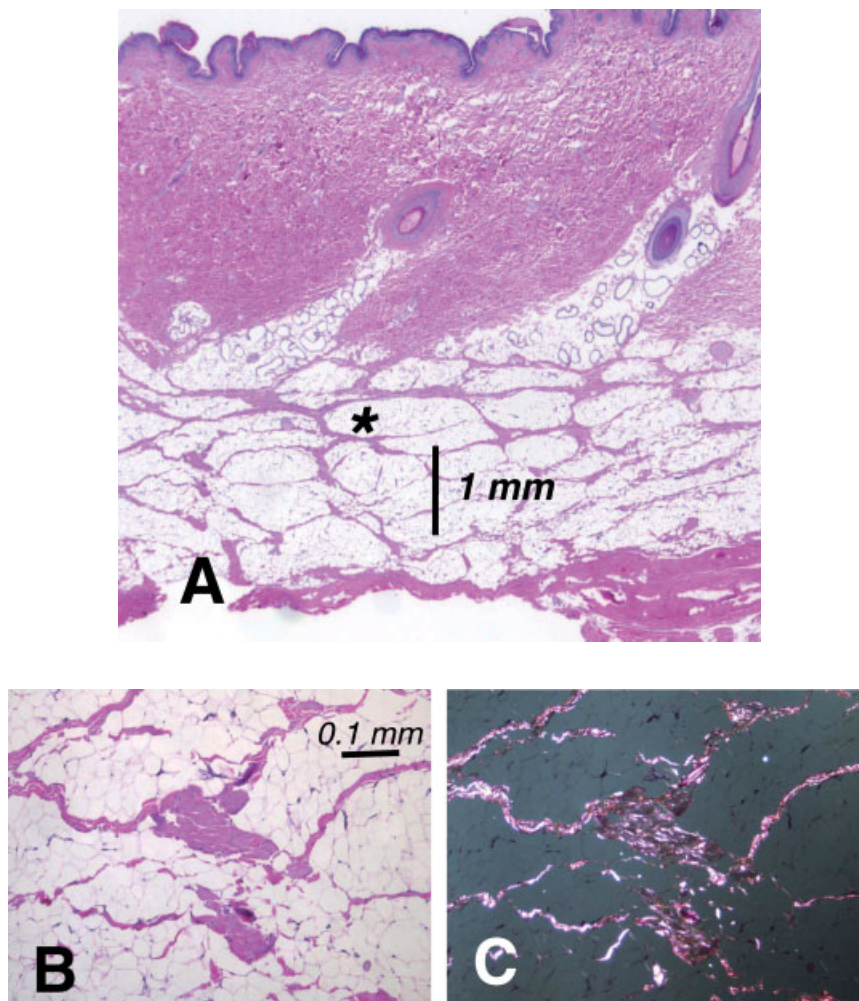


Fig. 5. Light microscopy (H&E stain) of fresh whole porcine tissue exposed *in vitro* to FEL at wavelengths near 1,210 nm, showed preferential injury of subcutaneous fat. Sample (A) exposed to 1,214 nm, 7.3 W/cm<sup>2</sup> irradiance for 16 seconds shows normal epidermis and dermis, with changes (\*) limited to the subcutaneous fat. In the fat, fibrous septae show hyalinization with altered staining, shown in (B). Focal loss of optical birefringence is seen by polarized light microscopy (C), due to thermal denaturation of type I collagen.

hyperplasia, nevus sebaceous, or rhinophima. The size and depth of sebaceous glands, suggest that they could be targeted by SP using 0.1–1 seconds pulses delivered with skin cooling. Sebaceous glands synthesize squalene and other lipids in addition to the triglycerides that predominate in fat, and the infrared absorption properties of sebocytes may differ considerably from those of adipocytes. However, it is clear that good contrast of infrared vibrational modes exists between sebaceous glands and the surrounding dermis. In a recent report, coherent anti-Stokes Raman spectroscopic (CARS) microscopy was performed *in vivo* to visualize cutaneous sebaceous glands [20]. The CARS microscope selectively excited vibrational modes of CH<sub>2</sub> in sebaceous glands. Our study also suggests that the 1,720 nm lipid-selective band may be useful for some superficial targets (up to

~2 mm deep) such as superficial sebaceous glands, xanthelasma, or fatty atheromatous plaque. Other lipid absorption bands including the very weak one at 915 nm, and the stronger modes at longer wavelengths may also be useful.

Finally, it should be noted that the superconducting FEL used in this study is a uniquely capable photon source for biomedical research. Jefferson National Laboratory's FEL emits tunable radiation from ultraviolet through far infrared wavelengths, at extremely high average power, in a train of femtosecond-domain micropulses. By returning otherwise-wasted electron energy back to the accelerator, this FEL operates efficiently and reliably. The device should be quite useful for action spectra, laser surgical, multiphoton excitation, and spectroscopy in biomedical systems.

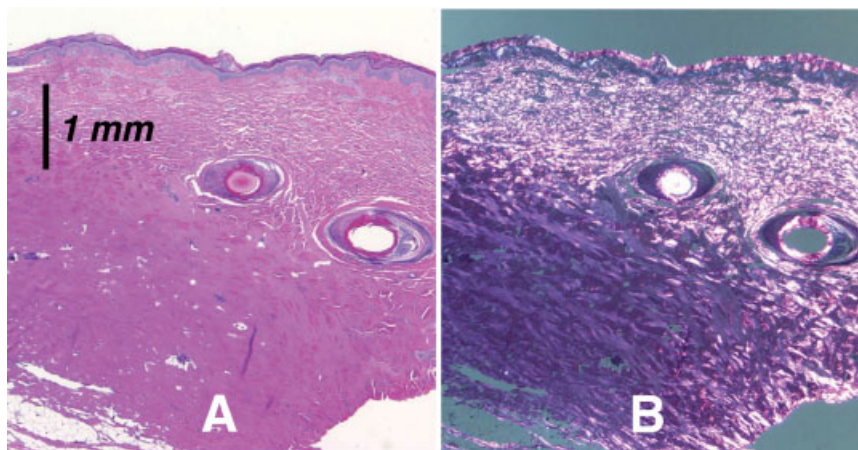


Fig. 6. Tissue damage from FEL exposures at 1,250 nm, a wavelength at which fat and dermis have equal photothermal excitation, always included dermal injury (H&E stain). This sample exposed at 1,250 nm, 20 W/cm<sup>2</sup> for 8 seconds shows extensive dermal and subcutaneous fat injury (A), with loss of optical birefringence (B). Lower FEL power produced less injury, but preferential injury of fat was never seen at this wavelength.

## ACKNOWLEDGMENTS

This work was supported in part by Department of Defense grant FA 9550-04-1-0079 of the Medical Free Electron Laser program; by the Office of Naval Research; and by Commonwealth of Virginia. The authors thank John Demir and Thomas Flotte MD for assistance with processing the pathological specimens.

## REFERENCES

- Parrish JA, Anderson RR. Selective photothermolysis: Precise microsurgery by selective absorption of pulsed radiation. *Science* 1983;220:524–527.
- Altshuler GB, Anderson RR, Manstein D, Zenzie HH, Smirnov MZ. Extended theory of selective photothermolysis. *Lasers Surg Med* 2001;29(5):416–432.
- Zenzie HH, Altshuler GB, Smirnov MZ, Anderson RR. Evaluation of cooling methods for laser dermatology. *Lasers Surg Med* 2000;26(2):130–144.
- Rothfleisch JE, Kosann MK, Levine VJ, Ashinoff R. Laser treatment of congenital and acquired vascular lesions [review]. *Dermatologic Clinics* 2000;20(1):1–18.
- Suzuki H, Anderson RR. Treatment of melanocytic nevi [review]. *Dermatol Therapy* 2005;18(3):217–226.
- Zelickson BD, Mehregan DA, Zarrin AA. Clinical, histological, and ultrastructural evaluation of tattoos treated with three laser systems. *Lasers Surg Med* 1994;15:364–372.
- Grossman MC, Dierickx C, Farinelli WA, Flotte TJ, Anderson RR. Damage to hair follicles by normal-mode ruby laser pulses. *J Am Acad Dermatol* 1996;35:889–894.
- Latina MA, deLeon JM. Selective laser trabeculoplasty [review]. *Ophthalmol Clin N Am* 2005;18(3):409–419.
- Zeitels SM, Franco RA, Dailey SH, Burns JA, Hillman RE, Anderson RR. Office-based treatment of glottal dysplasia and papillomatosis with the 585 nm pulsed dye laser and local anesthesia. *Ann Otol Rhinol Laryngol* 2004;113(4):265–276.
- Du Y, Hu XH, Cariveau M, Ma X, Kalmus GW, Lu JQ. Optical properties of porcine skin dermis between 900 nm and 1500 nm. *Phys Med Biol* 2001;46(1):167–181.
- van Veen RLP, Sterenborg HJCM, Pifferi A, Torricelli A, Chikoidze E, Cubeddu R. Determination of visible near-IR absorption coefficients of mammalian fat using time and spatially resolved diffuse reflectance and transmission spectroscopy. *J Biomed Opt* 2005;10(5):054004.
- Balasubramaniam TA, Bowman HF. Thermal conductivity and thermal diffusivity of biomaterials: A simultaneous measurement technique. *J Biomech Eng* 1977;99:148–154.
- Manstein D, Erofeev AV, Altshuler GB, Anderson RR. Selective photothermolysis of lipid-rich tissue. *Lasers Surg Med Suppl* 2001;13:6 (abstract).
- Neumann RA, Knobler RM, Pieczkowski F, Gebhart W. Enzyme histochemical analysis of cell viability after argon laser-induced coagulation necrosis of the skin. *J Am Acad Dermatol* 1991;25:991–998.
- Anderson RR, Beck H, Bruggemann U, Farinelli W, Jacques SL, Parrish JA. Pulsed photothermal radiometry in turbid media: Internal reflection of backscattered radiation strongly influences optical dosimetry. *Applied Optics* 1989;28:2256–2262.
- Edwards G, Logan R, Copeland M, Reinisch L, Davidson J, Johnson B, Maciunas R, Mendenhall M, Ossoff R, Tribble J. Tissue ablation by a free-electron laser tuned to the amide II band. *Nature* 1994;371:416–419.
- Matarasso A, Pfeifer TM. Mesotherapy for body contouring [review]. *Plast Reconstr Surg* 2005;115(5):1420–1424.
- van Vliet M, Ortiz A, Avram MM, Yamauchi PS. An assessment of traditional and novel therapies for cellulite [review]. *J Cosmetic Laser Ther* 2005;7(1):7–10.
- Mawafy M, Cassens RG. Microscopic structure of pig skin. *J Animal Sci* 1975;41(5):1281–1290.
- Evans CL, Potma IO, Puoris'haag M, Cote D, Lin CP, Xie XS. Chemical imaging of tissue in vivo with video-rate coherent anti-Stokes Raman scattering microscopy. *Proc Natl Acad Sci* 2005;102(46):16807–16812.